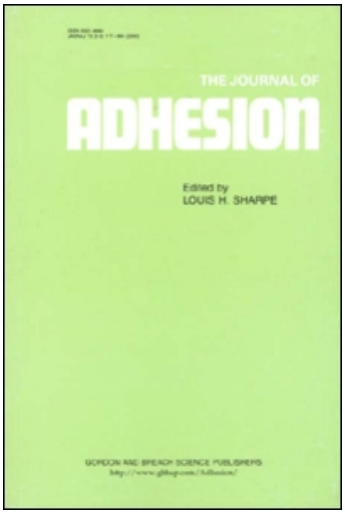

The Journal of Adhesion
Publication details, including instructions for authors and subscription information:
http://www.informaworld.com/smpp/title~content=t713453635

Pressure-sensitive adhesion in the blends of poly(N-vinyl pyrrolidone) and poly(ethylene glycol) of disparate chain lengths

Anna A. Chalykh[a]; Anatoly E. Chalykh[a]; Mikhail B. Novikov[b]; Mikhail M. Feldstein[b]
[a] Institute of Physical Chemistry, Russian Academy of Sciences, Moscow, Russia [b] A.V. Topchiev Institute of Petrochemical Synthesis, Russian Academy of Sciences, Moscow, Russia

Online publication date: 08 September 2010

To cite this Article Chalykh, Anna A. , Chalykh, Anatoly E. , Novikov, Mikhail B. and Feldstein, Mikhail M.(2002) 'Pressure-sensitive adhesion in the blends of poly(N-vinyl pyrrolidone) and poly(ethylene glycol) of disparate chain lengths', The Journal of Adhesion, 78: 8, 667 — 694
To link to this Article: DOI: 10.1080/00218460213491
URL: http://dx.doi.org/10.1080/00218460213491

The Journal of Adhesion, 78: 667–694, 2002

0021-8464/02 $12.00 +.00
DOI: 10.1080/00218460290010395

PRESSURE-SENSITIVE ADHESION IN THE BLENDS OF POLY(N-VINYL PYRROLIDONE) AND POLY(ETHYLENE GLYCOL) OF DISPARATE CHAIN LENGTHS

Anna A. Chalykh
Anatoly E. Chalykh
Institute of Physical Chemistry, Russian Academy of Sciences, Moscow, Russia

Mikhail B. Novikov
Mikhail M. Feldstein
A.V. Topchiev Institute of Petrochemical Synthesis, Russian Academy of Sciences, Moscow, Russia

Adhesive behavior in blends of high molecular weight poly(N-vinyl pyrrolidone) (PVP) with a short-chain, liquid poly(ethylene glycol) (PEG) has been studied using a 180° peel test as a function of PVP–PEG composition and water vapor sorption. Hydrophilic pressure-sensitive adhesives are keenly needed in various fields of contemporary industry and medicine, and the PVP–PEG adhesive hydrogels are among this specific class of materials. In PVP–PEG blends, pressure-sensitive adhesion has been established to appear within a narrow composition range, in the vicinity of 36 wt% PEG, and it is affected by the blend hydration. Both plasticizers, PEG and water, behave as tackifiers (enhancers of adhesion) in the blends with glassy PVP. However, PEG alone is shown to account for the occurrence of adhesion, and the tackifying effect of PEG is appreciably stronger than that of sorbed water. Blend hydration enhances adhesion for the systems that exhibit an apparently adhesive type of debonding from a standard substrate (at PEG content less than 36 wt%), but the same amounts of sorbed water are also capable of depressing adhesion in the PEG-overloaded blends, where a cohesive mechanism of adhesive joint failure is typical. The PVP-PEG blend with 36% PEG couples both the adhesive and cohesive mechanisms of bond rupture (i.e., the fibrillation of adhesive polymer

Received 3 December 2001; in final form 27 February 2002.

The research described in this publication was in part made possible by Award No. RC1-2057 of the U.S. Civilian Research & Development Foundation (CRDF). The authors thank Nicolai A. Platé, Costantino Creton, and Ronald A. Siegel for helpful discussion and stimulating advice.

Address correspondence to Mikhail M. Feldstein, A. V. Topchiev Institute of Petrochemical Synthesis, Russian Academy of Sciences, 29, Leninsky Prosp., 119991, Moscow, Russia. E-mail: mfeld@ips.ac.ru

under debonding force and predominantly adhesive locus of failure). Blend hydration effect on adhesion has been found to be reversible.

The micromechanics of adhesive joint failure for PVP–PEG hydrogels involves the fibrillation of adhesive polymer, followed by fibrils stretching and fracturing as their elongation attains 1000–1500%. Peel force to rupture the adhesive bond of PVP–PEG blends increases with increasing size of the tensile deformation zone, increasing cohesive strength of the material, and increasing tensile compliance of the material, obeying the well-known Kaelble equation, derived originally for conventional rubbery pressure-sensitive adhesives. The major deformation mode upon peeling the PVP–PEG adhesive from a standard substrate is extension, and direct correlations have been established between the composition behaviour of peel strength and that of the total work of viscoelastic strain to break the PVP–PEG films under uniaxial drawing. As a result of strong interfacial interaction with the PET backing film, the PVP–PEG adhesive has a heterogeneous two-layer structure, where different layers demonstrate dissimilar adhesive characteristics.

Keywords: Poly(N-vinyl pyrrolidone); Poly(ethylene glycol); Pressure-sensitive adhesion; Hydrogen bonding; Hydrogels; Effects of composition and hydration

INTRODUCTION

Pressure-sensitive adhesives (PSAs) are well known and have been used for many years in a variety of industrial, consumer, and medical applications [1]. The PSAs are characterized as being normally tacky and exhibiting instant tack when applied to a substrate. Many polymers have been used to produce PSAs including, for example, acrylic and methacrylic ester homo- or copolymers, butyl rubber-based systems, silicones, urethanes, vinyl esters and amides, olefin copolymer materials, natural or synthetic rubbers, and the like [1]. Most of the elastomers used to formulate PSAs exhibit viscoelastic properties typical of rubbers.

Among other applications, the PSAs are critical components of drug delivery systems, serving both as the means of device attachment to patient skin or mucosal tissues and a reservoir vehicle controlling the rate of drug delivery [2]. The following four major performance properties of PSAs constitute a basis for their application in drug-loaded adhesive patches:

1. *Adhesive*: High tack coupled with an optimum slip-stick transition point.
2. *Transport*: Drug-release kinetics controlled in terms of transdermal delivery rate and the functional lifetime of the device.
3. *Reservoir*: Drug compatibility and ability to be stored in a stable form tailored to the incorporated drug of interest.
4. *Biological*: No toxicity, skin irritation, or sensitization.

Because pressure-sensitive adhesion is a complex phenomenon, and the interrelationship between adhesive and transport properties remains insufficiently explored, the above-mentioned performance properties are difficult to combine in a single system. Therefore it is no wonder that there are only four major types of medical-grade PSAs: natural and synthetic rubbers, polyisobutylene (PIB), polydimethyl siloxane (PDMS), and acrylates. It is pertinent to note that currently available medical-grade adhesives are hydrophobic polymers [2].

For many pharmaceuticals, the solubility of the active agent in the reservoir of a transdermal drug delivery device is of decisive importance. With higher solubility, it is possible to increase the rate of transdermal delivery. Because many therapeutic agents are ionogenic organic substances having a higher solubility in hydrophilic media than in lipophilic vehicles, adhesive reservoirs based on hydrophilic polymers would be more versatile than those based on hydrophobic polymers. Other general advantages of hydrophilic adhesives are as follows:

1. Hydrophilic adhesives can provide greater adhesion to skin compared with hydrophobic adhesives, because the surface energy of hydrophilic adhesives is typically higher than that of hydrophobic polymers [3]. The hydrophobic PSAs have surface energies closer to that of biological substrates such as skin and mucosal membranes (22–30 mJ/m^2 [4–6]).
2. Hydrophilic adhesives are compatible with a wide variety of drugs, excipients, and additives due to the existence of specific polymer–additive interactions such as electrostatic and hydrogen bonding.
3. The plasticizing effect of water sorbed by hydrophilic adhesives from hydrated skin or mucosal tissues enhances adhesion, in contrast to hydrophobic adhesives.
4. The enhanced solubility of drugs in hydrophilic adhesives facilitates control over drug release kinetics.
5. With adhesives based on hydrophilic polymers, there is an expanded capability to control and manipulate the adhesive-cohesive balance.
6. The adhesive properties of hydrophilic polymers are considerably less sensitive to their molecular weight than those of hydrophobic polymers, as a result of intermolecular association of macromolecules containing complementary functional groups within hydrophilic adhesives.

Mixing polymers is a well-recognized method to obtain new polymer materials with tailored performance properties. Usually, the

composite properties are intermediate between those of the unblended polymers. New properties result generally from strong, specific interactions between polymeric components [7]. None of the existing hydrophilic individual polymers exhibit tack in a dry, unblended state, and tailoring hydrophilic PSAs is therefore a problem of special interest and great severity. A PSA hydrogel based on blends of high molecular weight poly(N-vinyl pyrrolidone) (PVP) with short-chain poly(ethylene glycol) (PEG) has been originally developed specifically for transdermal systemic delivery of drugs spanning a wide range of chemical structures and therapeutic categories [8–10]. Both PVP and PEG contain only electron-donating functional groups in their repeating units. For this reason, the PVP is reported to be immiscible both with high molecular weight poly(ethylene oxide) [11] and PEG, whose terminal hydroxyls are replaced by inert ester groups [12, 13]. However, the PVP has been found to be soluble in short-chain PEG [14], and this behavior is due to the contribution of PEG proton-donating terminal hydroxyl groups, which form hydrogen bonds to the complementary carbonyl groups in the repeating units of longer PVP chains [13, 15]. Since every PEG molecule bears two reactive OH groups at the chain ends, in an H-bonded PVP–PEG complex nearly 20–30% of PVP units have been found to be crosslinked into the H-bonding network through comparatively short and flexible PEG chains [12, 13]. Because the amount of H-bond crosslinked PVP units is independent of blend composition within a wide PEG concentration range, the PVP–PEG complex is stoichiometric [12, 13, 16].

Both PVP and PEG are capable of absorbing water as a vapor from the surrounding atmosphere. At ambient conditions (20–22°C and 50% relative humidity), PVP sorbs 6–13% water, whereas PEG hydration ranges from 1 to 1.5%. Normally, PVP–PEG blends contain from 4 to 10% water that is mainly associated with PVP and serves as an aid in PVP–PEG complex formation [17, 18]. In this way, the PVP–PEG blends are in essence ternary and can be considered as hydrogels. Adhesive properties of the hydrogels can therefore be affected not only by the PVP–PEG composition but also by the degree of hydration. Detailed characteristics of these effects are the primary focus of this work. Both effects must be intently analyzed to gain a molecular insight into the origin of the observed adhesion upon blending the hydrophilic polymers. This insight is of great importance in tailoring the adhesive properties of polymeric blends. The latter problem is a major and ultimate objective of our research, outlined in part in other relevant publications [8, 19–27].

MATERIALS AND METHODS

PVP ($M_w = 1{,}000{,}000$ g/mol) and PEG ($M_w = 400$ g/mol) were obtained from BASF as Kollidon K-90 and Lutrol E-400, respectively. Both polymers were used as obtained. Adhesive films 250–300 μm in thickness were prepared by dissolving the PVP and PEG in a common solvent (ethyl alcohol) followed by casting the solution on a poly(ethylene terephthalate) (PET) backing film 20 μm in thickness and drying for 3 days at ambient temperature (20–22°C). The films were then dried for 2 h under vacuum, at 65°C. The adhesives were saturated with water by equilibrating in dessicators with controlled pressure of water vapor at ambient temperature for 6–7 days. The equilibrium hydration of PVP–PEG adhesive films ranged from 5 to 30%. Unsupported adhesive films 700 μm in thickness were produced by casting the solution onto a PEBAX-600 release liner (0.6 mm in thickness) and drying for 3 days at ambient temperature. A uniform thickness of the PVP–PEG films was produced using the BYK-Gardner film casting knife. After blend drying the release liner was removed and unsupported PVP–PEG films were used in tensile test experiments.

The adhesive joint strength of PVP–PEG hydrogels was evaluated by 180° peel testing using an Instron 1221 Tensile Strength Tester at the peeling rate of 10 mm/min. A low-density polyethylene (PE) film of 100 μm in thickness, crystallinity ~45%, surface energy 28.5 mJ/m^2, was employed as a standard substrate. The time to attain a maximum strength of adhesive contact with the substrate was 20 min. This dwell time on the PE substrate prior to peeling has been found to be sufficient to provide the maximum strength of the adhesive bond for all the PVP–PEG blends examined in this work. The character of the adhesive joint failure was observed with a TV camera interfaced to an IBM computer and photographed with a microscope. The locus of failure was ascertained by contact angle measurement of the detached substrate surface. For this purpose, the contact angles of the PE substrate prior to contact with PVP–PEG adhesive and upon debonding were measured using a set of standard liquids: water, glycerol, PEG, tricresyl phospate, dodecane, and hexadecane. The contact angle of water with the PE substrate was found to be 98 ± 0.5°. Upon detachment of the PVP–PEG adhesive under adhesive debonding, this angle averaged 96°.

Tensile strain-stress behavior of the PVP–PEG films was studied with an Instron 1222 Tensile Tester at ambient temperature (20–22°C). The tensile strength of the samples was determined at fixed cross head speed ranging from 10 to 100 mm/min, 10 N full scale

load for the PVP–PEG hydrogel ranging in hydration from 3.5 to 6.5 wt%, and 4 N for the hydrogel containing 11 wt% of water. Dumbbell-shaped samples 21 mm in total length, with a nip-to-nip distance of 10 mm were cut from rectangular films 0.5–0.7 mm in thickness. The width of a necked region was 5 mm. All reported stress-strain curves were reproduced in replicate experiments, varying less than 10%, the ultimate tensile strength (σ_b) being the maximum force applied (to breaking) divided by the cross-sectional area of the sample. Elongation at break (ε_b) is calculated by dividing the distance that the crosshead of the Instron tensile tester had traveled to sample break by the original length of the sample. Tensile strain, ε, is determined by the increase in sample length (Δl) divided by its original length, l_o. Nominal tensile stress is defined as a stretching force normalised by the original cross-section area of the sample. Although the stress-strain curves are shown in this work in terms of nominal tensile stress, those were recalculated into true tensile stress values, and all the quantities, presented below, relate to true values. True tensile stress was calculated as the product of nominal stress by absolute elongation.

The locus of cohesive failure within the PVP–PEG adhesive film was quantitatively evaluated by sequential peeling of the adhesive layer (coated onto PET backing film) from PE substrate. Separated joints were weighed in closed bottles, and adhesive remainders at the substrate and backing film were determined. The peel stripping cycles were repeated with fresh substrate until termination in weight change.

RESULTS AND DISCUSSION

Effects of PVP–PEG Blend Composition and Hydration on Peel Strength

Being composed of typical hydrophilic polymers, PVP–PEG compatible blends absorb a large amount of water when exposed to water vapor at various relative humidities (RH), giving the isotherms presented in Figure 1. As a rule, the higher the PEG content the higher the hydration, especially at higher RH. Unblended PVP is evidently an outlyer of this rule, and a characteristic shoulder on the PVP isotherm within the lower RH region relates traditionally to the polymer hydration degree at which the PVP transition from glassy to rubbery state occurs [28, 29]. Annealing the PVP at 200°C, followed by slow cooling with a rate lower than $1°C/min^{-1}$, has been shown to cause the low p/p_s shoulder to vanish but does not affect appreciably the rapid growth in water uptake in the upper RH region. We attribute this observation to the presence of a thermal-history-dependent, unrelaxed hole-free volume in glassy PVP, within which the sorbed water may be accumulated [30].

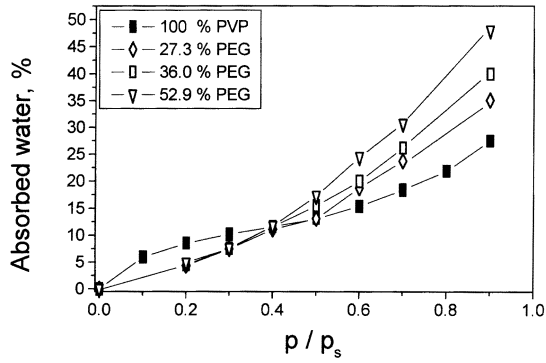

FIGURE 1 Water vapour absorption isotherms for PVP and its blends with PEG-400 at ambient temperature.

Although neither PVP nor PEG per se demonstrate any pressure-sensitive adhesion, their blends exhibit adhesion, and absorbed water can influence the adhesive behavior of the PVP–PEG hydrogels in a complicated manner, as is shown in Figures 2–4. In fact, only the blends in a very narrow range of PEG content (in the vicinity of 36 wt%) and RH (between 50 and 65%) provide high adhesion,

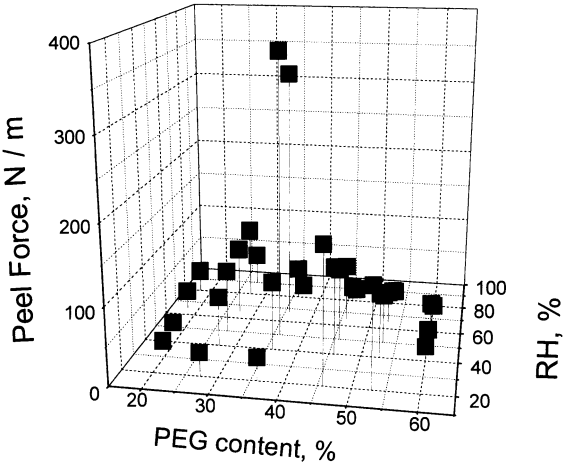

FIGURE 2 Effects of PEG content and relative humidity on 180° peel force to rupture adhesive joint of PVP–PEG hydrogel with PE film at ambient temperature. Peel rate 10 mm/min.

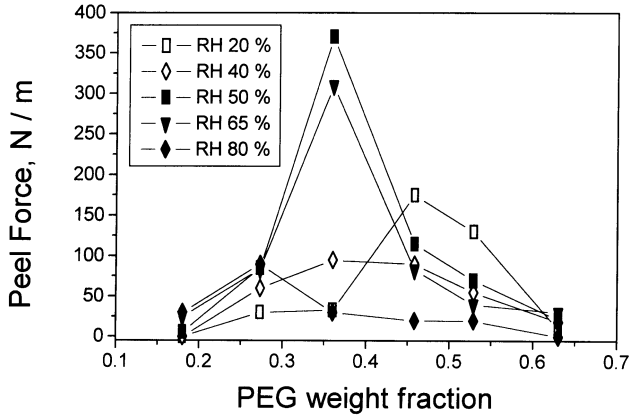

FIGURE 3 Adhesion of PVP–PEG blends as a function of PEG concentration at fixed relative humidities of surrounding atmosphere.

whereas both PEG-underloaded and overloaded blends reveal no or insignificant adhesion, demonstrating that both of the individual polymers are non-adhesive. Actually, the blend containing 36% PEG provides adhesion that is nearly three times as great as the maximum adhesion for the blends of any other composition. This behavior makes the PVP–PEG system a very convenient model from which to elicit the molecular structure responsible for pressure-sensitive adhesion. For this purpose, we have to compare the structure and properties of

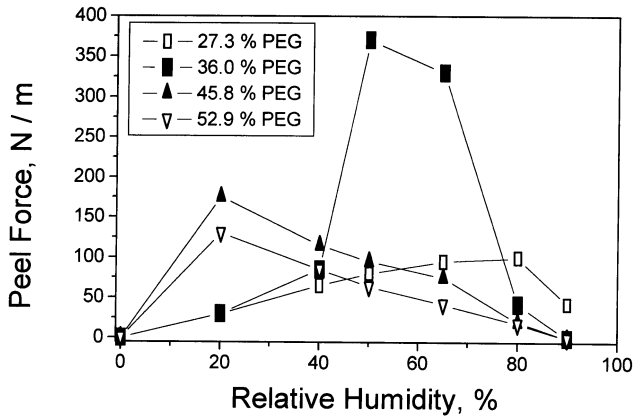

FIGURE 4 Impact of relative humidity upon adhesive behavior of PVP–PEG blends.

adhesive and nonadhesive PVP–PEG blends. This issue is analyzed in detail in other works [19–27, 31]. With the growth of the content of both plasticizers (PEG and water), the mode of adhesive joint failure changes from adhesive to cohesive. The maximum peel strength at 36% PEG corresponds to a transition point.

As is evident from Figures 2–4, water absorption causes opposite effects on the adhesion of PEG underloaded (27.3%) and overloaded (45.8 and 52.9%) blends. Water vapor absorption is associated with a significant plasticizing action of water, as reflected by appreciable reduction in the glass transition temperature of PVP and PVP–PEG blends [15–17]. The left-hand (ascending) branch of the curves in Figures 3 and 4 correspond to compositions in the immediate vicinity of the glass transition, and water behaves there as a plasticizer by shifting the PSA rheology into a viscoelastic state, resulting in an enhancement of adhesion. By contrast, for rubbery blends in the right-hand (descending) branches of the plots, water serves as a cosolvent and contributes to a reduction of adhesive toughness by decreasing the cohesive strength of hydrogels. As is evident from Figure 2, PEG and water are equally critical in obtaining a high peel adhesion, because both binary PVP blends, with PEG and with water, reveal no adhesion, and only ternary PVP–PEG–water blends are adhesive. Both plasticizers, PEG and water, account for the PVP blends' adhesive properties, affecting critically the height and position of the peel force maximum along the axis of PEG and water content. For the substrates and peeling rates employed for monitoring the PVP–PEG hydrogel adhesive properties, the maximum strength always occurs when the blend contains 36 wt% PEG. The PEG overloaded blends (45.8 and 52.9% PEG) exhibit maximum adhesion at lower RH (20%), whereas the blend containing 27.3% of PEG forms the strongest adhesive joint at 80% humidity. Relatively dry blends (at RH = 20%) require more PEG to be sufficiently plasticized in order to provide strong adhesive bonds. Although short-chain PEG has been shown to be a significantly more potent plasticizer for PVP compared with water [16], their plasticizing effects are additive and complement each other (Figure 5). For this reason, when the peel force is plotted against weight fraction of combined plasticizer ($w = w_{PEG} + w_{H_2O}$), all the data points from Figures 2–4 are mainly fit by the curves with a maximum at 36% PEG content (Figure 5).

With increasing time of PVP–PEG hydrogel contact with PE substrate the adhesion rises, gradually attaining its limiting value in 15–20 min (Figure 6). Although the time required to form the bond is a function of PVP–PEG composition and water content, the maximum dwell time (20 min) is needed for the blend containing 36% PEG,

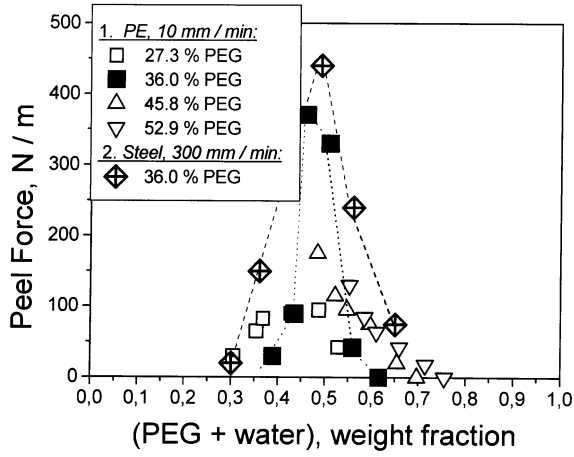

FIGURE 5 Generalized dependence of adhesive joint strength for PVP–PEG hydrogels of different compositions on the weight fraction of combined plasticizer (PEG + water).

equilibrated to 50% RH and absorbing 13% water. The adhesives with lower and higher levels of PEG and water than the adhesive of Figure 6 require shorter times to form the bond. The time required to form the bond is very much dependent not only on the specific adhesive formulation and rheology but also on the type of adhesive joint failure. As

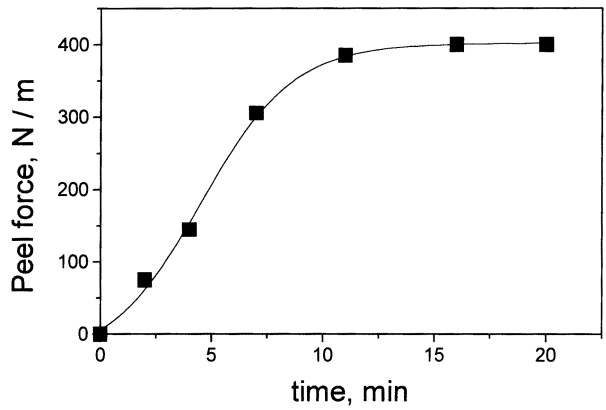

FIGURE 6 Adhesive bonding kinetics to PE substrate for the PVP–PEG hydrogel, containing 36 wt% PEG-400, exposed to RH = 50% and absorbing 13% water.

is shown above, this blend corresponds to the transition between adhesive and cohesive mechanisms of debonding. For this reason, we always evaluated the peeling force after 20 min of contact. This time is generally considered to be required in order to form an adhesive-substrate interfacial zone [32–34]. In addition, we have recently established a direct correlation between the kinetics of PVP–PEG hydrogel relaxation at the stage of polymer creep recovery upon the removal of the adhesive-bonding compressive force and the kinetics of adhesive strength growth shown in Figure 6 [35].

The blend hydration effect on adhesion has been found to be reversible. For the cohesive type of debonding, even a very slight hydration of the adhesive layer (by breathing) during peeling causes an immediate drop in the detaching force. On the contrary, blend dehydration by equilibrating the adhesive to lower relative humidity of the surrounding atmosphere leads to an increase in adhesion (Figure 7). In contrast, in the case of adhesive failure the plasticization of PVP–PEG blend by hydration results in the enhancement of peel strength, whereas dehydration produces a gradual loss of tack and adhesion.

Fracture Mechanics of Adhesive Joints

While knowledge of the above-reported dependence of PVP–PEG adhesive hydrogel peel strength on composition and hydration is quite essential to elicit the molecular origin of adhesion in hydrophilic

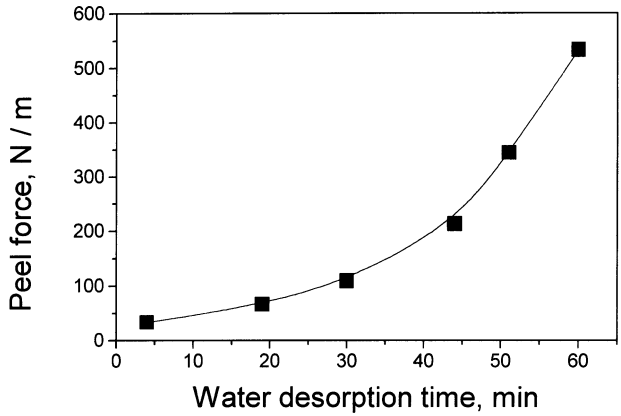

FIGURE 7 Effect of PVP–PEG (36 wt%) hydrogel dehydration on peel strength of adhesive joints with PE substrate.

polymer blends, it provides only limited information. In order to gain a better and quantitative understanding of this problem the mechanism of debonding must be taken into consideration.

Detailed observations of the deformation zone during peeling, assigned to relevant points in the force-displacement curves (Figure 8), provide valuable information on the mechanism of adhesive joint fracture. As is shown by the changes in contact angles on the substrate surface before bonding and after adhesive joint failure, at the microscopic level the locus of failure is always cohesive for PVP–PEG PSA. In terms of the adhesive remainder at the substrate surface the debonding can be defined either as predominantly adhesive (Type I) for PVP-rich and dry blends corresponding to the left-hand (ascending) branches of the curves in peel strength-composition (hydration) plots (Figures 3, 4), or as cohesive for PEG-rich and hydrated blends for right-hand (descending) branches and the transition point at maximum strength of the adhesive bond observed for the PVP blend with 36% PEG at RH = 50% (Type II) (see also Figures 3 and 4). As is established by the examination with an electron microscope of the substrate surface upon debonding, small fragments of adhesive fibrils (approximately 0.5–1.0 μm in length and 0.05–0.1 μm in diameter) are observed on the substrate surface, causing the change in contact angle. This type of debonding we define as predominantly adhesive. These observations are in a good compliance with recently reported

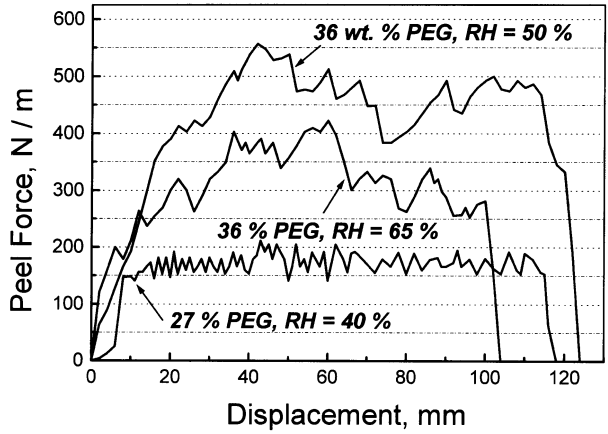

FIGURE 8 Load versus displacement traces of PVP–PEG hydrogel adhesive joint failure with PE substrate. I, 27% PEG, RH = 40%; II, 36% PEG, RH = 65%; III, 36% PEG, RH = 50%.

results of the probe tack testing of the PVP–PEG adhesives containing 31, 36, and 41% PEG and 11% water [31]. In terms of locus of failure, all adhesives except the 41% PEG at a low debonding rate (2 μm/s and lower) failed apparently adhesively, i.e., no optically detectable residue of adhesive was found on the probe after the test was completed.

The Type I peel force-debonding front displacement curves in Figure 8 have a sawtooth shape characteristic of a stable, brittle failure. The PVP–PEG hydrogel behaves here as a plastic in the vicinity of the glass transition temperature (T_g) that has been shown to be close to ambient temperature for PVP-overloaded and dry blends [12, 15, 16]. At the transition point (Type II) the adhesive demonstrates maximum peel strength and the properties of a rubber-like elastomer [15, 36]. The T_g for the blends in the transition point ranges between −40 and −55°C. We define the transitional type of bond fracture as a coupling of adhesive fibrillation under debonding stress (that is typical of cohesive debonding) with predominant rupture of the fibrils at the adhesive-substrate interface ("adhesive" locus of failure). For the PVP blend with 36% PEG at RH = 50% the failure mode changes from adhesive to cohesive, and there is a concomitant change in the peel character from shocky peel to smooth peel (Figure 8). The teeth become significantly wider, smoother and sparser, and the number of notches between them relates approximately to the number of voids optically visible in the stretched adhesive film under peeling. Apart from these cavities the peel strength is invariant with displacement. For conventional PSAs, the transition from smooth peel character to shocky peel character (as the peel rate increases or the temperature of the PSA is decreased or the T_g of the PSA is increased) is observed at a slip-stick point. It is typically not associated with a transition from adhesive to cohesive failure as it is for the PVP–PEG hydrogels. The Type II behavior is also peculiar to an adhesive of enhanced fluidity due to increased content of plasticizers (PEG, water). A decrease in viscosity with higher plasticizer content leads to a reduction in peel force required to rupture the adhesive bond [15], and cohesive failure is observed.

Debonding of pressure-sensitive adhesives in peel or probe tack tests has been reported to occur not through the initiation and propagation of cracks in the plane of the adhesive layer along the PSA-substrate interface but rather through the formation of fine fibrils in the tensile direction which are progressively extended, spanning a joint prior to its complete separation [31, 37]. Depending on the angle at which a tape is peeled, the fibrils may consume a reasonable portion of the force required to remove adhesive tape from a substrate. This general mechanism is typical of the PVP–PEG PSA joint fracture as well

[26, 31], exhibiting several important peculiarities. Those are readily visible under microscopic observation of the debonding process in the course of peel testing (Figures 9 and 10). Like other PSAs, long and large cavities are disposed within the PVP–PEG hydrogel in the plane normal to the adhesive layer, but those are comparatively few and far between, whereas the walls between the voids are much thicker and can be defined as drawing rods rather than the fine fibrils (Figure 9). As a result, the PVP–PEG adhesive joints fail by elastic stretching of adhesive bulk up to a critical value of tensile strain of $\varepsilon = 1000-1500\%$, where a fracture occurs. The entire layer of the adhesive is thus subjected to elongational flow in fibrils, providing resistance to detaching and energy dissipation. The viscoelastic deformation of the adhesive in extension is a major energy-dissipating mechanism, and the energy mainly dissipates in a region close to the front of joint separation where ε attains its maximum value at fracture, ε_f.

Figure 10 illustrates how the debonding process looks in the plane of separation of a backing film and substrate. The layer of intact adhesive is seen here as a light band at the border between a darker

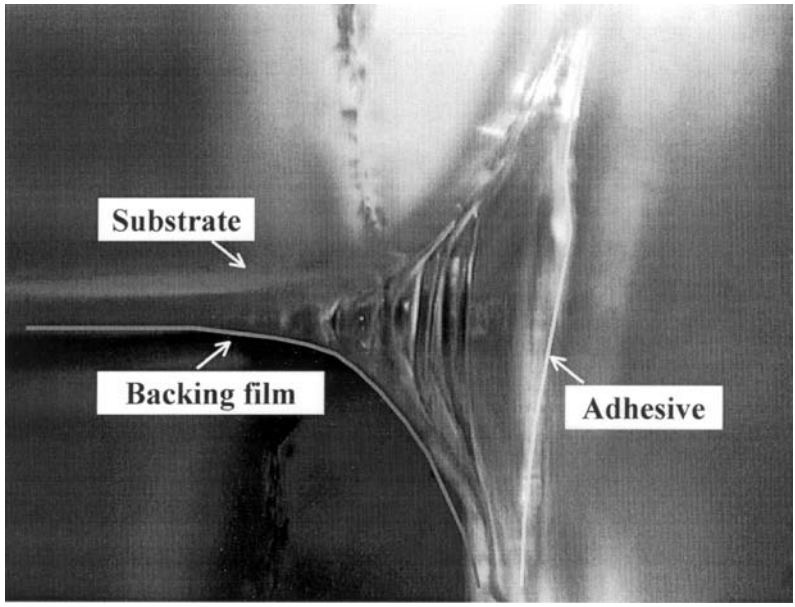

FIGURE 9 A photomicrograph of PVP–PEG (36 wt%) hydrogel adhesive joint failure with PE substrate viewed from the side. Initial thickness of adhesive layer is 250 μm. Prior to bonding the PVP–PEG adhesive was exposed to RH = 50% and absorbed 13% water.

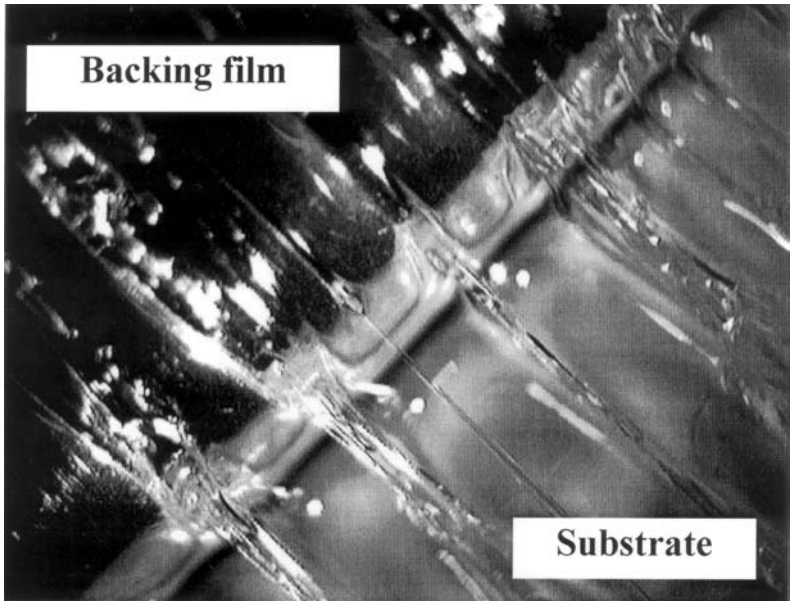

FIGURE 10 Front view of PVP–PEG (36 wt%) hydrogel adhesive joint failure with PE substrate. Prior to bonding the PVP–PEG adhesive was exposed to RH = 50% and absorbed 13% water. Intact adhesive layer of 250 μm in thickness is seen as a light band between backing film and substrate.

adhesive layer and lighter substrate. Adhesive joint fracture mechanics involves fibrillation of the adhesive layer. The length of extended fibrils is 10–20 times greater than the thickness of the intact adhesive layer. The fibrils are located throughout the entire width of adhesive film at nearly equal intervals. This fact implies that a mechanism of fibril nucleation is not random and that the adhesive material is spatially arranged into a three-dimensional network. Physically this conclusion seems to be fairly reasonable, because the existence of a PVP–PEG H-bonded rubber-like network is well documented at both molecular (FTIR spectroscopy) and macroscopic (rheology) levels [13, 15, 36]. More comprehensive data on the micromechanics of the PVP–PEG adhesive cavitation and fibrillation during probe tack testing are reported in our recent paper [31]. Indeed, the parallel geometry of flat-ended probe tests is better adapted to study the details of the debonding mechanisms of soft deformable adhesives than the geometry provided by peel testing [31, 37].

The locus of failure may be established by examining the fibril necking (Figure 10). The necks are shifted towards the substrate,

indicating that failure occurs in the region that is closer to the substrate surface than to the backing film. This means that the locus of failure is cohesive. Indeed, as follows from an electron microscopic investigation of the substrate surface upon debonding, adhesive remainder on the backing film is appreciably larger than that on the substrate surface. This finding was also confirmed by the increase of PE substrate surface energy upon adhesive joint separation.

To gain a quantitative insight into the mechanism of PVP–PEG hydrogel adhesive joint fracture, the stress-strain analysis of the debonding process under peeling is helpful.

In the course of peeling, the tensile stress, σ, is nonuniformly distributed within the deformation zone (Figures 9, 11). Let us denote the length of strained region by y and assume that it consists of the range of unit increments, dy, each being subjected to peeling force (P) which develops tensile stress, σ_i, and strain, ε_i. Along the whole length of the strained region, y, the adhesive stress and strain increase steadily from 0 up to critical values of σ_f and ε_f, where a fracture occurs:

$$P = b \int_0^y \frac{\sigma_i(y)}{2} dy, \tag{1}$$

where b is the width of the adhesive joint. Since the further away a current point in the strained region is removed from intact adhesive layer, the larger the tensile strain, it is logical to assume a proportionality between y and the extension of adhesive layer, Δl:

$$y = k \cdot \Delta l = k \cdot l \cdot \varepsilon_f, \tag{2}$$

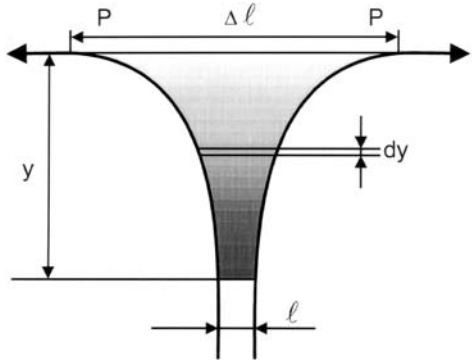

FIGURE 11 Schematic representation of adhesive joint fracture.

where $0 \leq k \leq 1$ and l is the thickness of adhesive layer. Within the intact adhesive layer $k = 0$, and at the point of fracture $k = 1$. Substituting Equation (2) into Equation (1) gives

$$P = k \cdot b \cdot l \int_0^{\varepsilon_f} \frac{\sigma(\varepsilon)}{2} d\varepsilon, \tag{3}$$

where the integral is the specific work of the viscoelastic stretching of the adhesive layer to rupture an adhesive joint, which is identical to the work of adhesion. Within the framework of the linear-elastic fracture mechanics (LEFM) approach, the specific work of viscoelastic deformation and fracture of the adhesive layer may be expressed through the critical values of ultimate stress, σ_f, and strain, ε_f, at fracture:

$$P = \frac{k \cdot b \cdot l \cdot \sigma_f \cdot \varepsilon_f}{2}. \tag{4}$$

Finally, if adhesive joint fracture occurs within the linear-elastic strain region:

$$P = \frac{k \cdot b \cdot l \cdot \sigma_f^2}{4E}, \tag{5}$$

where E is the tensile modulus of adhesive. If the peel force, P, is used to evaluate the adhesive joint strength at cohesive or miscellaneous type of fracture, the k value may be taken equal to unity, because adhesive toughness is mainly governed at cohesive debonding by the stress at the point of fracture:

$$P = \frac{b \cdot l \cdot \sigma_f^2}{4E}. \tag{6}$$

This expression is identical to the Kaelble equation, derived originally to describe the PSA time-temperature relationship of 180° peeling force [38, 39], and corresponds to the equation for adhesive fracture energy, G_a, derived from the consideration of the LEFM model of crack propagation by plastic deformation and yielding of adhesive ahead of the crack tip [3],

$$G_a = \frac{2\pi \cdot r \cdot \sigma_y^2}{E}, \tag{7}$$

where r is the radius of the plastic deformation zone and σ_y is the uniaxial yield stress of adhesive that is elastic up to this stress and then becomes plastic. The models outlined by Equations (6) and (7) demonstrate that the toughness of an adhesive joint increases with the

rise of plastic or elastic tensile cohesive strength of a polymer, the size of plastic or tensile deformation zone, and an increase in polymer tensile compliance.

Correlation between Peel Strength and the Fracture Characteristics of PVP – PEG Adhesive Films under Uniaxial Extension

The Kaelble Equation (6) holds for high angle peel, where a shear mechanism is reported to be negligible and the tensile strain dominates [39]. Since the established type of adhesive layer deformation is extension (Figures 9 and 10), it is logical to search for correlations between the composition dependencies of adhesive and tensile behavior of PVP–PEG hydrogels in the process of peeling and uniaxial drawing, respectively. This approach is considered to be quite productive in order to verify the validity of our assumption, made in the course of Equation (6) derivation, that the peel behavior of PVP–PEG adhesive can be described adequately within the framework of the LEFM model.

Actually, at first glance the use of the LEFM framework to describe the deformation of pressure-sensitive adhesives may seem like a dubious exercise. Pressure-sensitive adhesives work because they are not linear elastic in nature. Rather they are nonlinear viscoelastic liquids. The PSAs need to dissipate energy in a viscous manner in order to perform well. While the blends having low PEG and low water contents may behave more closely to a linear elastic fashion, the more heavily plasticized blends (high PEG and water content) would certainly be expected to exhibit a large viscous flow component during peeling. As has been recently established by comparing the tack and the small-strain linear viscoelastic properties of PVP–PEG blends [31], these adhesives show a large level of decoupling between their adhesive behavior and the small-strain linear viscoelasticity. As a result it is impossible to predict even qualitatively adhesive properties from the small-strain G' and G'' data in stark contrast with conventional PSA. At the same time, an obvious correlation has been found between the tack of PVP–PEG adhesives and their large-strain tensile properties [31, 40, 41].

This is because two different networks occur in PVP–PEG blends. The first network is mainly associated with longer PVP chains and is provided by their entanglements. The second network results from H-bonding of the hydroxyl groups on both ends of shorter PEG macromolecules to the carbonyls in PVP repeat units, which leads to the PVP crosslinking through PEG chains. The contribution of the first

network prevails in a small-strain linear elastic region, whereas the H-bonded network controls the large-strain viscoelastic properties of the PVP–PEG adhesives.

In order to show the validity of Equations (4) to (6) and demonstrate how far the stress-strain curves depart from linear elastic behavior, we should verify whether the product of an ultimate stress by a break elongation can approximate adequately the work of extension to break the PVP–PEG adhesive.

Figure 12 illustrates the effect of PEG content on the stress-strain behavior of PVP–PEG blends under drawing with a fixed extension rate of 10 mm/min. The shape of the stress-strain curves is typical of rubbery polymers. Transition from ductile strain and fracture with fibril formation (typical of the PVP blend with 41% PEG that deforms like an uncrosslinked viscoelastic liquid) to the brittle-like fracture (inherent in the PVP blend with 31% PEG, which strains like a cured rubber) occurs mainly within a narrow range of PVP–PEG composition. The blend containing 36 wt% PEG exhibits tensile behavior which is just intermediate between that of PEG-underloaded (31%) and overloaded (41%) compositions. It is pertinent to recall that during peel testing the brittle-like behavior (revealed by the blend containing 31 wt% PEG) is associated with an adhesive type of debonding. The ductile strain involving the fibrillation is typical of cohesive failure and high tack, exemplified by the blend containing 41% PEG.

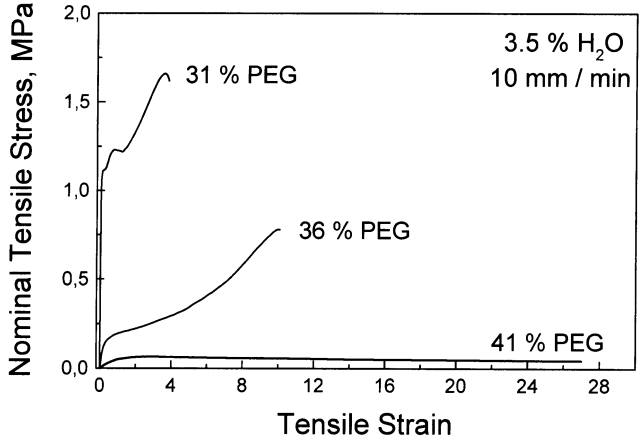

FIGURE 12 Tensile stress-strain curves for PVP blends of 3.5% hydration with 31, 36, and 41 wt% of PEG-400 under uniaxial drawing to break with a rate of 10 mm/min.

Respectively, the PVP blend with 36 wt% PEG has been found to manifest the transitional type of adhesive bond fracture. This transition results in coupling of adhesive fibrillation under debonding stress (that is typical of cohesive debonding) with predominant rupture of the fibrils at the adhesive-substrate interface (adhesive locus of failure). In the transition point, the intermolecular interaction forces within the adhesive polymer are properly counterbalanced by the force of adhesive-substrate interaction.

The ductile deformation found for the PVP blend with 41% PEG has been shown to be a characteristic feature of PSAs made from a blend of an elastomer and a tackifier, such as the mixture of a high and low molecular weight polyisobutylene [40]. The distinctive feature of tensile straining, found for the elastomer/tackifier blends (PSAs) containing significant amounts of low molecular weight tackifiers (which dilute the chain entanglements of the elastomer), is a comparatively small ultimate strength coupled with a large break elongation value. Comparing the tensile and peel behavior of PVP blends with different contents of PEG, we see that the PEG behaves as an adhesion enhancer. Actually, this conclusion is confirmed by direct probe tack measurements [26, 31].

It might be worth emphasizing the distinction between the PVP–PEG adhesive and classic rubber/tackifier PSA systems. The rubbers have low T_g values that are increased by addition of tackifier while the plateau modulus is decreased. For the PVP–PEG hydrogels, the base polymer, PVP, has a high T_g, and the PEG or water decreases the T_g and plateau modulus simultaneously [31]. Although these additives produce tack, they are not acting as "tackifiers" in the classical sense because they do not increase T_g. Instead, they are acting strictly as plasticizers. The fact that the PEG produces a higher deformation work at a given T_g than the lower-molecular-weight water plasticizer, resulting in higher peel force [40, 41], is a useful point to make.

It is well recognized that the macroscopic properties of polymer materials, such as adhesion and viscoelasticity, are a function of their molecular structure. Despite evident distinction between the composition and properties of the PVP–PEG adhesive and classical PSAs, we believe that similar features govern their adhesive behavior at a very fundamental, molecular level. In this connection, the molecular insight into the rheological and adhesive properties of the PVP–PEG system is of great importance.

Tensile testing provides the following characteristics of material fracture: break elongation (ε_b), ultimate stress (σ_b), and the total work of viscoelastic strain to break a polymer under uniaxial drawing (W_b).

The ε_b value is an indirect measure of molecular mobility in the adhesive polymer [27, 40, 41]. The higher the free volume within PVP–PEG blends, evaluated with Positron Annihilation Life-Time Spectroscopy, the greater the ε_b [27]. At the same time, the σ_b value is a direct measure of the cohesive strength of the polymer material. While the σ_b and ε_b values relate mainly to the moment of break, the W_b quantity is a characteristic of the overall process of polymer straining up to fracture. The latter value is plotted in Figure 13 against the PEG concentration in PVP blends along with the 180° peel force to rupture the PVP–PEG hydrogel adhesive bond to the PE substrate. The W_b value is outlined by the area under the tensile stress-strain curves shown in Figure 12.

The work of adhesion in Equation (3) is defined as the energy required to separate an interface reversibly. At cohesive failure, the two phases are identical, and the integral term in Equation (3) is the work of adhesive polymer cohesion. Taking into consideration that under cohesive failure the fracture energy dissipates mainly due to the tensile deformation of PVP–PEG hydrogel (Figures 9 and 10), it is reasonable to expect a close correlation between the total work of viscoelastic strain to break a stretched adhesive polymer film (W_b), outlined by the area under tensile stress-strain curves to draw and break the adhesive polymer (Figure 12), and the work of PVP–PEG hydrogel cohesion, embedded in Equation (3).

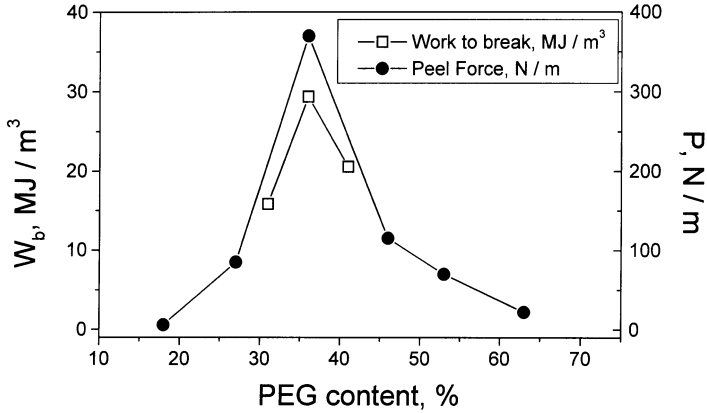

FIGURE 13 The composition plot of peel force, P, to rupture the PVP–PEG hydrogel adhesive bond toward polyethylene substrate and the work of viscoelastic strain to break the hydrogel film under stretching with a rate of 10 mm/min, W_b.

The fundamental physical significance of the W_b value invokes, eventually, the product of cohesive interaction energy and the free volume (that, in turn, determines a molecular mobility) within the polymer subjected to uniaxial drawing [41]. It is just this fundamental quantity that has been shown earlier to control the behavior of adhesion with the composition of PVP–PEG blends [19, 20, 23–25]. It is therefore not surprising that the W_b compositional dependence follows the pattern of peel adhesion and exhibits a maximum at 36% PEG concentration (Figure 13).

The physical meaning of this observation is that the PVP blend with 36% PEG dissipates maximum viscoelastic energy under uniaxial stretching, and that the tensile deformation mode governs the adhesive bond fracture mechanics under the 180° peel test. In the PVP blend with 31% PEG-400 there is a lack of ductility and molecular mobility, which prevents the development of sufficiently high break elongation. In contrast, within the blend containing 41% PEG the molecular mobility is high, but the lack of cohesive strength does not allow development of a sufficiently high value of ultimate tensile stress at polymer break. The PVP blend with 36% PEG demonstrates the best coupling of the cohesive interaction energy and the molecular mobility.

The PVP dissolution in PEG is a two-stage process [42]. At high PVP concentrations, the PEG plasticizing effect occurs, and the glass transition temperature of the blend drops dramatically, over 220°C, manifesting large negative deviations from the values found with a simple weight-average rule of mixing. This stage is due to the PVP–PEG stoichiometric network complex formation, where the PVP repeating units are crosslinked by H-bonding through both PEG terminal OH groups [12]. At higher PEG concentrations, the PVP–PEG network complex swells and dissolves gradually in excess solvent (short-chain, liquid PEG), and at this stage the PVP–PEG interaction has been shown to be comparatively weaker [42]. As follows from the data in Figure 14, at the first stage of PVP dissolution in PEG (the stage of stoichiometric complex formation), the PEG acts as both a plasticizer and cohesive strength enhancer, increasing the ultimate tensile stress at break (σ_b). In contrast, at the second stage of PVP dissolution, the solvent (PEG) acts only as diluent and plasticizer, decreasing the cohesive strength evaluated in terms of the σ_b value. The implication of this fact is that at PEG concentrations less than 36% the short-chain PEG plasticizing effect is coupled with H-bonding and crosslinking of longer PVP chains through both PEG terminal hydroxyl groups [12]. Upon the achievement of the critical 36% concentration, the PEG behaves only as a plasticizer and terminates PVP

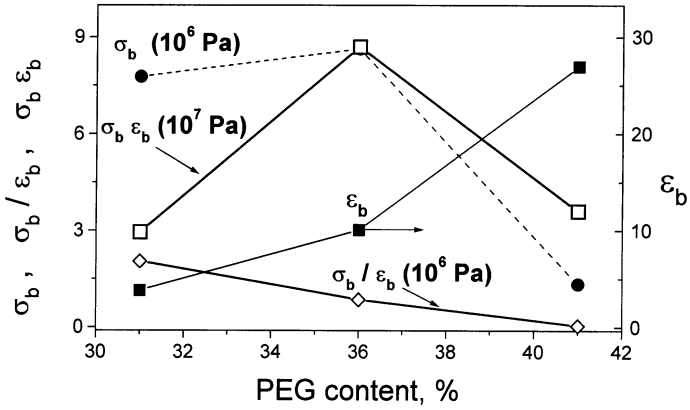

FIGURE 14 Relationship of ultimate tensile stress (σ_b) and maximum elongation at break (ε_b), their product and ratio to the content of PEG-400 in the blends with PVP of 3.5% hydration. Extension rate is 10 mm/min.

H-bond curing. Plasticizing and tackifying effects of PEG are demonstrated by the growth of elongation at break (ε_b) with PEG concentration (Figure 14).

In the context of tensile strain–peel adhesion correlations, a question is pertinent: whether the $(\sigma_b \cdot \varepsilon_b)/2$ quantity can approximate adequately the total deformation work to break the PVP–PEG hydrogel under uniaxial stretching. In the plan of adhesive behavior, the resolution of this issue can shed light upon applicability of the Kaelble Equation (4) for peel force in the PVP–PEG system. The Kaelble equation in the form similar to the expressions in Equations (4) and (6) also describes the force required to break the film of a rubber-like polymer under uniaxial drawing [38]. Similar to the compositional plot of the total deformation work in Figure 13, the $\sigma_b \cdot \varepsilon_b$ product goes through a maximum at 36 wt% PEG concentration (Figure 14). As the data in Figure 15 show, being plotted against the W_b values for the blends of various hydration and PEG content, the $\sigma_b \cdot \varepsilon_b$ product exhibits a straight line with a slope of 2.39 ($R = 0.989$, $p < 0.0001$). If the PVP–PEG hydrogel tensile strain behavior obeyed a linear elasticity law, with a tensile modulus invariable in the course of elongation, the $\sigma_b \cdot \varepsilon_b$ product would be twice as large as the total deformation work (see Equation (4)). Thus, in PVP–PEG blends the $\sigma_b \cdot \varepsilon_b$ product is about 20% larger than might be predicted with Equation (4), and the difference between the obtained and predicted values is the result of tensile strain deviations from an ideal linear elastic behavior.

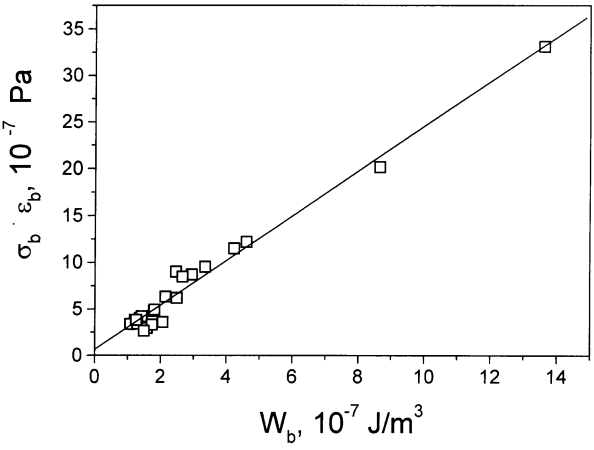

FIGURE 15 Relationship between the total deformation work to break the PVP–PEG hydrogels of different hydration and PEG content (W_b) and relevant values of the $\sigma_b \cdot \varepsilon_b$ product.

The total deformation work to break the adhesive polymer film and the $\sigma_b \cdot \varepsilon_b$ product outlines a specific coupling of the cohesive energy and free volume (molecular mobility) as a descriptor of viscoelastic and adhesive behaviour of PVP–PEG hydrogel. However, while other fundamental quantities—such as the glass transition temperature and the change in heat capacity at the glass transition—have embedded the combination of the contributions of cohesion and free volume, the tensile test data allow us to estimate each of these contributions separately in terms of σ_b and ε_b values. Consequently, we can evaluate not only the product of cohesive and free volume contributions but also their ratio, σ_b/ε_b. This ratio is plotted against the PVP–PEG blend composition in Figure 14 and exhibits a monotonous decrease with the rise in PEG content. A formal physical significance of the σ_b/ε_b ratio is an apparent ultimate tensile modulus at the moment of polymer fracture. As the data in Figure 14 indicate, the maximum energy that has to be expended in order to draw and break a unit volume of PVP–PEG hydrogel ($\sim 4-9 \times 10^7$ J/m^3) corresponds to the apparent ultimate tensile modulus $\sigma_b/\varepsilon_b \approx 2-9 \times 10^5$ Pa, and these two magnitudes refer to the composition of the PVP–PEG stoichiometric complex which provides best adhesion (Figures 2 and 3). Let us recall the well-known Dahlquist criterion of tack, defining the elasticity modulus of various pressure-sensitive adhesives in the order of 10^5 Pa [43]. Although the chemical composition and structure of PVP–PEG hydrogel are absolutely dissimilar compared with

those for conventional pressure-sensitive adhesives, nevertheless the PVP–PEG H-bonded network also obeys the Dahlquist criterion of tack, and this fact allows us to appreciate the physical meaning of this phenomenological criterion. At a most fundamental, molecular level, the Dahlquist criterion of tack specifies the ratio between cohesive interaction energy and free volume within pressure-sensitive adhesive polymers.

Locus of Failure, Interfacial Interaction and Structure of PVP–PEG Adhesive Layer

In order to evaluate quantitatively the locus of failure within the PVP–PEG adhesive, the adhesive layer was removed from the PET-backing film by sequential stripping with a fresh PE substrate, and the weight of adhesive remaining after the separation of the adhesive joint was determined both at the backing film and the substrate. The results for the peeling test at the rates of 10 and 50 mm/min are presented in Figure 16.

During the first and second stripping, approximately 30 and 25 wt% of adhesive is transferred from backing film to substrate, indicating that the locus of failure is shifted toward the substrate surface. The amount of stripped adhesive increases with debonding rate decrease.

At the same time, after the third stripping the adhesive remaining on the backing film ceases to vary, approaching a limit ranging from 20

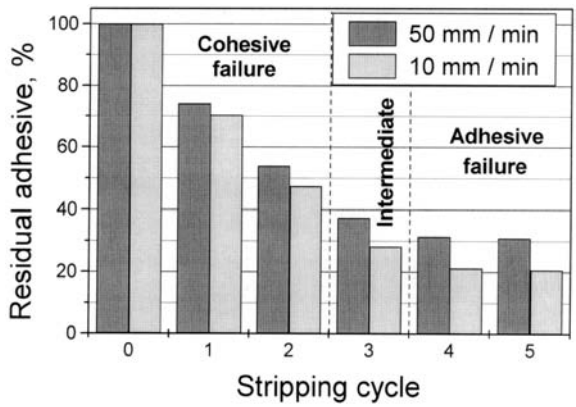

FIGURE 16 Remainder of PVP–PEG (36% PEG, RH = 50%) adhesive hydrogel at PET-backing film (wt%) upon sequential stripping of adhesive layer with PE substrate; peel rate 10 and 50 mm/min. The blend hydration was 13%.

to 30% depending on the debonding rate. The unremovable adhesive layer demonstrates dissimilar adhesive characteristics as compared with the intact PVP–PEG adhesive. Adhesion towards the PET-backing film becomes very strong in comparison with the adhesion toward the PE substrate, and the mode of failure changes from cohesive to adhesive. The locus of the adhesive debonding within the removable layer is shifted toward the backing film with each subsequent stripping.

What is the nature of the unremovable adhesive layer at the interface with the backing film? We have found that if the same PET film is used both as backing film and the substrate for PVP–PEG adhesive hydrogel, adhesion toward the PET substrate is significantly less than that toward the PET-backing film. It means that the reason is not in the nature of substrate and backing, but rather in the difference of hydrogel-bonding procedures with PET film employed as the substrate and backing. The adhesive bonding of PVP–PEG hydrogel with PET-backing film is provided by casting the PVP–PEG solution followed by the removal of solvent with drying. In the solvent, the PVP–PEG hydrogel is highly swollen. Upon drying, the adhesive bonds arise between the hydrogel and backing film, which prevent the swollen hydrogel from shrinkage. As the result, at the interface with PET-backing film the hydrogel network is stretched, leading to additional, unrelaxed stress. This unrelaxed interfacial stress enhances the adhesion to PET backing, but reduces the adhesion at the opposite interface with PET substrate. In this way, the unremovable layer is formed. In turn, the outer surface of the PET-supported unremovable layer serves as a backing for the removable layer of relaxed PVP–PEG hydrogel, which exhibits high tack toward various substrates.

CONCLUSIONS

In the blends of high molecular weight, glassy PVP with a short-chain, liquid PEG adhesion appears in a narrow range of composition and hydration. The PVP blends with 36 wt% PEG have been shown to exhibit maximum adhesion and the proper balance of cohesive strength and interfacial interaction with the substrate (transition point). The blends containing lower PEG concentrations reveal adhesive type of debonding, whereas those overloaded with PEG demonstrate cohesive failure in the course of a 180° peel test. In the blends with glassy PVP, the PEG and sorbed water behave as adhesion enhancers and plasticizers within the entire composition range. Both are adhesion enhancers for the blends displaying the adhesive type of debonding (PVP content more than 64 wt%), and produce adhesion

decline once a cohesive failure is typical (at PEG content 36 wt% and higher).

Fracture mechanics of PVP–PEG adhesive joints obey the well-known Kaelble equation, derived originally for rubbery cross-linked PSAs. According to this equation, adhesion increases with increasing size of tensile deformation zone, cohesive strength of material, and its tensile compliance. At low peeling rates, the mechanism of PVP–PEG adhesive fracture involves the fibrillation of adhesive followed by the fibrils' extension and fracture as elongation attains 1000–1500%. The major type of adhesive film deformation under peeling is extension, and evident correlations have been found between the compositional behavior of peel force and the total work of viscoelastic tensile strain to break the adhesive polymer in the course of uniaxial drawing. As a result of interfacial interaction with the backing film, the PVP–PEG hydrogel consists of two layers having different adhesive characteristics.

REFERENCES

[1] Satas, D., Ed., *Handbook of Pressure-sensitive Adhesive Technology* (Satas & Associates, Warwick, RI, 1999) 3rd ed.

[2] Pfister, W. R., Adhesives and Requirements for Transdermal Drug Delivery, in Hadgraft, J. and Marty, J. P., Eds., *Development Issues in Transdermal Drug Delivery* (Controlled Release Society Workshop, Nice, France, 1994) Chap. 6.

[3] Kinloch, A. J., *Adhesion and Adhesives: Science and Technology* (Chapman and Hall, London, 1987).

[4] Schott, H., *J. Pharm. Sci.*, **60**, 1893–1895 (1971).

[5] Rosenberg, A., Williams, R., and Cohen, G., *J. Pharm. Sci.*, **62**, 920–922 (1973).

[6] Ginn, M. E., Dunn, S. C., and Jungermann, E., *J. Am. Oil Chem. Soc.*, **47**, 83–85 (1970).

[7] Paul, D. R., and Newman, S., *Polymer Blends* (Academic Press, NY, 1978).

[8] Feldstein, M. M., and Platé, N. A., in *NBC Risks*, Sohn, T., and Voicu, V. A., Eds., NATO Science Series: 1. Disarmament Technologies (Kluwer Academic Publishers, Dordrecht, 1999) Vol. 25, pp. 441–458.

[9] Feldstein, M. M., Tohmakhchi, V. N., Malkhazov, L. B., Vasiliev, A. E., and Platé, N. A., *Int. J. Pharm.*, **131**, 229–242 (1996).

[10] Feldstein, M. M., Raigorodskii, I. M., Iordanskii, A. L., and Hadgraft, J., *J. Control. Release*, **52**, 25–40 (1998).

[11] Cesteros, L. C., Quintana, J. R., Fernandez, J. A., and Katime, I. A., *J. Polym. Sci., Polym. Phys. Ed.*, **27**, 2567–2576 (1989).

[12] Feldstein, M. M., Kuptsov, S. A., Shandryuk, G. A., and Platé, N. A., *Polymer*, **42**, 981–990 (2001).

[13] Feldstein, M. M., Lebedeva, T. L., Shandryuk, G. A., Igonin, V. E., Avdeev, N. N., and Kulichikhin, V. G., *Polym. Sci.*, **41**(A), 867–875 (1999).

[14] Bairamov, D. F., Chalykh, A. E., Feldstein, M. M., Siegel, R. A., and Platé, N. A., *J. Appl. Polym. Sci.*, **85**, 1128–1136 (2002).

[15] Feldstein, M. M., Lebedeva, T. L., Shandryuk, G. A., Kotomin, S. V., Kuptsov, S. A., Igonin, V. E., Grokhovskaya, T. E., and Kulichikhin, V. G., *Polym Sci.* **41**(A), 854–866 (1999).

[16] Feldstein, M. M., Shandryuk, G. A., and Platé, N. A., *Polymer*, **42**, 971–979 (2001).
[17] Feldstein, M. M., Kuptsov, S. A., Shandryuk, G. A., Platé, N. A., and Chalykh, A. E., *Polymer*, **41**, 5349–5359 (2000).
[18] Vartapetian, R. Sh., Khozina, E. V., Kärger, J., Geschke, D., Rittig, F., Feldstein, M. M., and Chalykh, A. E., *Macromol. Chem. Phys.*, **202**, 2648–2652 (2001).
[19] Feldstein, M. M., Chalykh, A. E., Chalykh, A. A., and Platé, N. A., *Polym. Mater. Sci. Eng.*, **81**, 465–466 (1999).
[20] Feldstein, M. M., Chalykh, A. E., Chalykh, A. A., Fleischer, G., and Siegel, R. A., *Polym. Mater. Sci. Eng.*, **81**, 467–468 (1999).
[21] Chalykh, A. A., Chalykh, A. E., and Feldstein, M. M., *Polym Mater. Sci. Eng.*, **81**, 456–457 (1999).
[22] Chalykh, A. E., Chalykh, A. A., and Feldstein, M. M., *Polym Mater. Sci. Eng.*, **81**, 427–428 (1999).
[23] Feldstein, M. M., Chalykh, A. E., Vartapetian, R. Sh., Kotomin, S. V., Bairamov, D. F., Borodulina, T. A., Chalykh, A. A., and Geschke, D., *Proc. 23rd Annual Meeting Adhesion Soc.*, 54–56 (2000).
[24] Feldstein, M. M., Chalykh, A. E., and Platé, N. A., *Proc. 5th European Conference on Adhesion (EURADH'2000)*, Lyon, France, 176–181 (2000).
[25] Feldstein, M. M., Borodulina, T. A., Vartapetian, R. Sh., Kotomin, S. V., Kulichikhin, V. G., Geschke, D., and Chalykh, A. E., *Proc. 24th Annual Meeting Adhesion Soc.*, 137–139 (2001).
[26] Roos, A., Creton, C., and Feldstein, M. M., *Proc. 24th Annual Meeting Adhesion Soc.*, 277–279 (2001).
[27] Feldstein, M. M., Platé, N. A., Chalykh, A. E., and Cleary, G. W., *Proc. 25th Annual Meeting Adhesion Soc.*, 292–294 (2002).
[28] Zhang, J., and Zografi, G., *J. Pharm. Sci.*, **89**, 1063–1072 (2000).
[29] Gerasimov, V. K., Chalykh, A. A., Chalykh, A. E., Razgovorova, V. M., and Feldstein, M. M., *Polym. Sci.*, **43**(A), 1266–1271 (2001).
[30] Chalykh, A. E., Gerasimov, V. K., Razgovorova, V. M., Bairamov, D. F., Feldstein, M. M., and Siegel, R. A., *Proc. Intern. Symp. Control. Release Bioactive Mater.*, **27**, 690–691 # 7104 (2000).
[31] Roos, A., Creton, C., Novikov, M. B., and Feldstein, M. M., *J. Polym. Sci., Polym. Phys. Ed.*, submitted.
[32] Schnell, R., Stamm, M., and Creton, C., *Macromolecules*, **31**, 2284–2292 (1998).
[33] Schnell, R., Stamm, M., and Creton, C., *Macromolecules*, **32**, 3420–3425 (1999).
[34] Schnell, R., Lorenz-Haas, C., Stamm, M., and Creton, C., *Proc. 23rd Annual Meeting Adhesion Soc.*, 508–510 (2000).
[35] Chalykh, A. E., Chalykh, A. A., Bairamov, D. F., Borodulina, T. A., and Feldstein, M. M., *Proc. 23rd Annual Meeting Adhesion Soc.*, 127–128 (2000).
[36] Kotomin, S. V., Borodulina, T. A., Feldstein, M. M., and Kulichikhin, V. G., *Polym Mater. Sci. Eng.*, **81**, 425–426 (1999).
[37] Lacrout, H., Sergot, P., and Creton, C., *J. Adhesion*, **69**, 307–353 (1999).
[38] Kaelble, D. H., *Adhesive Age*, **3**(5), 37–40 (1960).
[39] Kaelble, D. H., in *Handbook of Pressure-sensitive Adhesive Technology*, Satas, D., Ed. (Satas & Associates, Warwick, RI, 1999) 3rd ed., Chap. 6, pp. 96−120.
[40] Novikov, M. B., and Feldstein, M. M., *Polymer* (submitted).
[41] Feldstein, M. M., Novikov, M. B., and Shandryuk, G. A., *Polymer* (submitted).
[42] Feldstein, M. M., *Polymer*, **42**, 7719–7726 (2001).
[43] Dahlquist, C. A., in *Treatise on Adhesion and Adhesives*, Patrick, R. L. Ed. (M. Dekker, NY, 1969) Vol. 2, p. 219–260.